

Transport and anisotropy in single-crystalline SrFe_2As_2 and $A_{0.6}\text{K}_{0.4}\text{Fe}_2\text{As}_2$ ($A=\text{Sr}, \text{Ba}$) superconductors

G. F. Chen, Z. Li, J. Dong, G. Li, W. Z. Hu, X. D. Zhang, X. H. Song, P. Zheng, N. L. Wang, and J. L. Luo
Beijing National Laboratory for Condensed Matter Physics, Institute of Physics, Chinese Academy of Sciences, Beijing 100190, China
 (Received 3 July 2008; revised manuscript received 28 October 2008; published 9 December 2008)

We have successfully grown high-quality single crystals of SrFe_2As_2 and $A_{0.6}\text{K}_{0.4}\text{Fe}_2\text{As}_2$ ($A=\text{Sr}, \text{Ba}$) using flux method. The resistivity, specific heat, and Hall coefficient have been measured. For parent compound SrFe_2As_2 , an anisotropic resistivity with ρ_c/ρ_{ab} as large as 130 is obtained at low temperatures. A sharp drop in both in-plane and out-plane resistivities due to the spin-density-wave (SDW) instability is observed below 200 K. The angular dependence of in-plane magnetoresistance shows twofold symmetry with field rotating within ab plane below SDW transition temperature. This is consistent with a stripe-type spin ordering in SDW state. In K-doped $A_{0.6}\text{K}_{0.4}\text{Fe}_2\text{As}_2$ ($A=\text{Sr}, \text{Ba}$), the SDW instability is suppressed and the superconductivity appears with T_c above 35 K. The rather low anisotropy in upper critical field between $H\parallel ab$ and $H\parallel c$ indicates that interplane coupling plays an important role in hole-doped Fe-based superconductors.

DOI: 10.1103/PhysRevB.78.224512

PACS number(s): 74.70.-b, 74.62.Bf, 74.25.Gz

The recent discovery of superconductivity with transition temperature $T_c \sim 26$ K in $\text{LaFeAsO}_{1-x}\text{F}_x$ has generated tremendous interest in scientific community.¹ Shortly after this discovery, the T_c was raised to 41–55 K by replacing La by rare-earth Ce, Sm, Pr, Nd, etc., making those systems with T_c exceeding 50 K.^{2–5} The undoped quaternary compounds crystallize in a tetragonal ZrCuSiAs -type structure, which consists of alternate stacking of edge-sharing Fe_2As_2 tetrahedral layers and La_2O_2 tetrahedral layers along c axis. Very recently, superconductivity with T_c of up to 38 K was discovered in AFe_2As_2 ($A=\text{Ba}, \text{Sr}, \text{Ca}$) upon K or Na doping.^{6–10} AFe_2As_2 compounds crystallize in a tetragonal ThCr_2Si_2 -type structure with identical Fe_2As_2 tetrahedral layers as in LaFeAsO , but separated by single elemental A layers. These compounds contain no oxygen in A layers. The simpler structure of AFe_2As_2 system makes it more suitable for research of intrinsic physical properties of Fe-based compounds.

Except for a relatively high transition temperature, the system displays many interesting properties. The existence of a spin-density-wave (SDW) instability in parent LaFeAsO (Ref. 11) was indicated by specific heat, optical measurements, and first-principles calculations, and subsequently confirmed by neutron-scattering,¹² NMR,¹³ μSR ,¹⁴ and Mössbauer¹⁵ spectroscopic measurements. The superconductivity only appears when SDW instability was suppressed by doping carriers or applying pressure. The competition between superconductivity and SDW instability was identified in other rare-earth substituted systems.^{2,16,17} Besides the SDW instability, structural distortions from tetragonal to monoclinic were also observed for both ReFeAsO ($\text{Re}=\text{rare earth}$) and AFe_2As_2 ($A=\text{Ba}, \text{Sr}, \text{Ca}$).^{18–23} The structural transition temperatures were found to occur at slightly higher than SDW transition temperature in LaFeAsO ,¹² but the two transitions occur simultaneously in AFe_2As_2 ($A=\text{Ba}, \text{Sr}, \text{Ca}$).^{18,19,24} The band-structure calculation and neutron-scattering experiments indicated a stripe-type antiferromagnetic structure of Fe moments in SDW state in LaFeAsO .^{11,12} In such a spin structure, a fourfold spin rotation symmetry is broken and reduced to twofold. It is interesting to see if such

a twofold symmetry could be observed in angular-dependent magnetoresistance (MR) measurements.

In this work, we present resistivity, specific-heat, and Hall-coefficient measurements on single crystals of SrFe_2As_2 and $A_{0.6}\text{K}_{0.4}\text{Fe}_2\text{As}_2$ ($A=\text{Sr}, \text{Ba}$). A large anisotropic resistivity with $\rho_c/\rho_{ab} \sim 130$ is observed for SrFe_2As_2 . Below 200 K, a sharp drop in both in-plane and out-plane resistivities due to the SDW instability is observed, similar to previous results on polycrystal samples.⁷ Moreover, the angular dependence of in-plane and out-plane magnetoresistances shows twofold symmetry with field rotating within ab plane below SDW transition temperature. The breaking of fourfold rotation symmetry to twofold provides transport evidence for the formation of a stripe-type antiferromagnetic structure of Fe moments in SDW state. Moreover, the anisotropy of upper critical field for high-quality single crystals of $\text{Sr}_{0.6}\text{K}_{0.4}\text{Fe}_2\text{As}_2$ is investigated. The interlayer coupling is relatively strong in superconducting samples.

The parent single crystals of SrFe_2As_2 were prepared by the high-temperature solution method using Sn as flux, similar to the procedure described in Ref. 21. The superconducting crystals $A_{0.6}\text{K}_{0.4}\text{Fe}_2\text{As}_2$ ($A=\text{Sr}, \text{Ba}$) were prepared by the high-temperature solution method using FeAs as flux. The starting materials of Sr or Ba, K, and FeAs in a ratio of 0.5:1:4 were put into an alumina crucible and sealed in welded Ta crucible under 1.6 atm of argon. The Ta crucible was then sealed in an evacuated quartz ampoule and heated at 1150 °C for 5 h and cooled slowly to 800 °C over 50 h. The platelike crystals with sizes up to 10 mm \times 5 mm \times 0.5 mm could be obtained after breaking the alumina crucible. Both scanning electron microscopy with energy dispersive x-ray (SEM/EDX) and induction-coupled plasma (ICP) analyses revealed that the elemental composition of the crystal is $A_{0.6\pm\delta}\text{K}_{0.4\mp\delta}\text{Fe}_2\text{As}_2$ ($A=\text{Sr}, \text{Ba}$) with $\delta \leq 0.02$. Figure 1(a) shows x-ray-diffraction pattern of parent SrFe_2As_2 with the 00 l reflections. The lattice constant $c=0.1239$ nm was calculated from the higher-order peaks, comparable to that of polycrystalline sample.⁷ Figure 1(b) shows the EDX analysis of $\text{Ba}_{0.6}\text{K}_{0.4}\text{Fe}_2\text{As}_2$ crystal.

The in-plane resistivity was measured by the standard

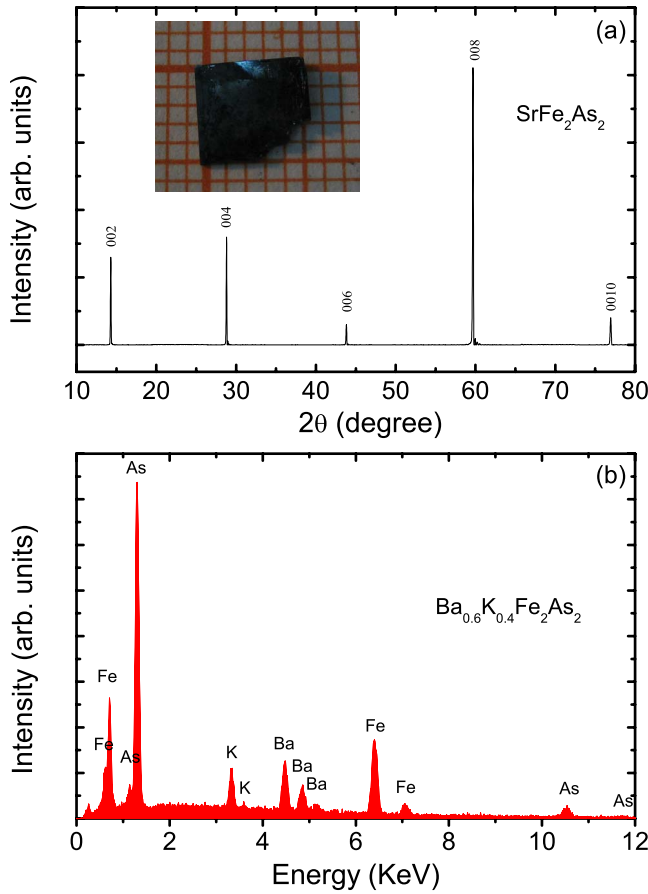


FIG. 1. (Color online) (a) Single-crystal x-ray-diffraction pattern for SrFe_2As_2 . The inset shows the photograph of a SrFe_2As_2 single crystal (length scale, 1 mm). (b) EDX analysis of $\text{Ba}_{0.6}\text{K}_{0.4}\text{Fe}_2\text{As}_2$ crystal.

four-probe method. The out-plane resistivity was measured using a typical method for layered materials as shown in inset of Fig. 2(b). The silver paste was used to cover almost all area of upper and lower sides of the measured sample for two current leads, and leaves two small holes in the center of both sides for the voltage leads. Assuming that the current density is uniformly distributed throughout the cross section, the resistivity can then be measured with $\rho_c = RS/d$, where R is the resistance, S is area of cross section, and d is the thickness of the sample. The error comes mostly from the measurement of geometry factors. The ac magnetic susceptibility was measured with a modulation field in the amplitude of 10 Oe and a frequency of 333 Hz. The Hall-coefficient measurement was done using a five-probe technique. The specific-heat measurement was carried out using a thermal relaxation calorimeter. All these measurements were performed down to 1.8 K in a physical property measurement system (PPMS) of Quantum Design company.

Figure 2(a) shows the temperature dependence of in-plane resistivity ρ_{ab} in zero field and 8 T, and Fig. 2(b) shows the out-plane resistivity ρ_c for SrFe_2As_2 in zero field. They have similar T -dependent behavior and exhibit a strong anomaly at about 200 K: the resistivity drops steeply below this temperature. This is a characteristic feature related to SDW instability and a structural distortion in parent compounds of

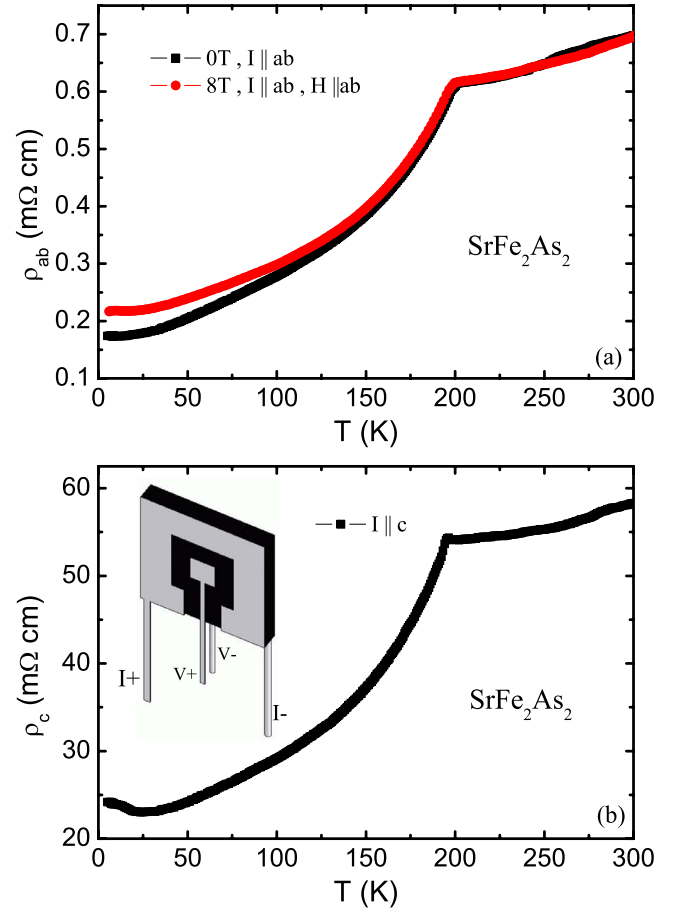


FIG. 2. (Color online) (a) The in-plane resistivity ρ_{ab} for SrFe_2As_2 in zero field and 8 T. (b) The out-plane resistivity ρ_c in zero field. The inset shows a sketch of how to measure ρ_c .

Fe-based high- T_c superconductors.^{11,12} The transition temperature is slightly lower than that observed in polycrystalline SrFe_2As_2 (~ 205 K). The anisotropic resistivity ρ_c/ρ_{ab} is found to be $\sim 130 \pm 65$ at 25 K. It is comparable with that of layered cuprates $\text{YBa}_2\text{Cu}_3\text{O}_{7-\delta}$.²⁵ From Fig. 2(a), we find that the SDW transition temperature is insensitive to the applied field; however a large positive magnetoresistance is observed at low temperatures. At 10 K, the magnetoresistance $[\rho_{ab}(8\text{ T}) - \rho_{ab}(0\text{ T})]/\rho_{ab}(0\text{ T})$ reaches as high as 25%. The behavior is similar to that observed in polycrystalline LaFeAsO .¹¹ The large positive magnetoresistance can be understood from the suppression of SDW order by applied field, and thus, the spin scattering is enhanced.

In a system with strong coupling of charge carrier and background magnetism, angular-dependent magnetoresistance (AMR) is a useful tool to detect the magnetic structure of background magnetism. AMR measurements have been successfully used in understanding the spin structure of slightly doped high- T_c cuprates and charge ordering $\text{Na}_{0.5}\text{CoO}_2$ systems.^{26,27} For this purpose, we measured the in-plane resistivity with magnetic field of 10 T rotating within the ab plane for SrFe_2As_2 . Figure 3 shows AMR $[\Delta\rho(\theta) = \rho(\theta) - \rho(90^\circ)]$ at 10, 30, 50, 100, 150, and 200 K. $\Delta\rho(\theta)$ shows a clear twofold oscillation below 200 K. However, the twofold oscillation disappears at 200 K, a tempera-

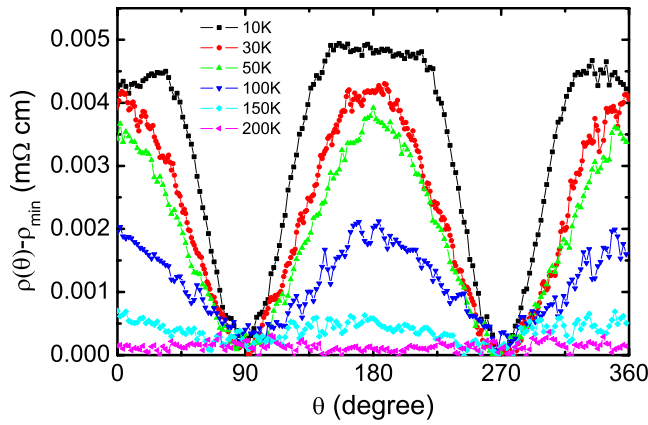


FIG. 3. (Color online) Angular dependence of in-plane magnetoresistance [$\Delta\rho(\theta) = \rho(\theta) - \rho(90^\circ)$] at different temperatures in external magnetic field of 10 T rotating within ab plane for SrFe_2As_2 .

ture just above T_{SDW} . Above T_{SDW} , the spin orientations of Fe moments are random so there is no angular-dependent magnetoresistance arising from spin scattering. However below T_{SDW} , a large MR is observed at low temperature and it originates from the enhanced spin scattering while SDW order is suppressed in external magnetic field. Therefore the symmetry of the AMR oscillation reflects directly the symmetry of spin structure. The observation of twofold-symmetry oscillations in SrFe_2As_2 in low temperatures indicates the stripe-type spin structure of Fe moments in ground state. The recent neutron-diffraction measurements on SrFe_2As_2 single crystals²⁴ and polycrystalline²⁸ indicate that the SDW transition is indeed presented in SrFe_2As_2 system below a transition temperature of $\sim 200\text{--}220$ K. The stripe-type antiferromagnetic spin structure is found in the SDW state. Moreover, the angular-dependent magnetization measurement on BaFe_2As_2 crystal with field rotating within the ab plane also shows a twofold symmetry of magnetization below SDW transition temperature,²⁹ consistent with the AMR measurements on SrFe_2As_2 crystals. Therefore AMR can act as a probe for SDW order in these systems without having to wait for neutron beam time. Similar twofold-symmetry oscillations of AMR have been observed in $\text{Na}_{0.5}\text{CoO}_2$, which was attributed to ordering of charge stripes.²⁷

To get more information about the SDW and structural phase transition, we performed specific-heat and Hall resistivity measurements for SrFe_2As_2 . Figure 4(a) shows the temperature dependence of specific heat C from 2 to 230 K. We can see clearly a sharp δ -function shape peak at about 200 K with $\Delta C \sim 185$ J/mol K. This is a characteristic feature of a first-order phase transition. The transition temperature agrees well with that observed in resistivity measurement. The latent heat of the transition is estimated as being 463 ± 50 J/mol by integrating the area of the specific-heat data around the transition peak after subtracting the background. The background is estimated using a linear fit of the specific-heat data above and below the transition. It is worth noting that only one peak at around 200 K is observed in SrFe_2As_2 , different from that of LaFeAsO where two subsequent peaks at 155 and 143 K were observed in specific-heat

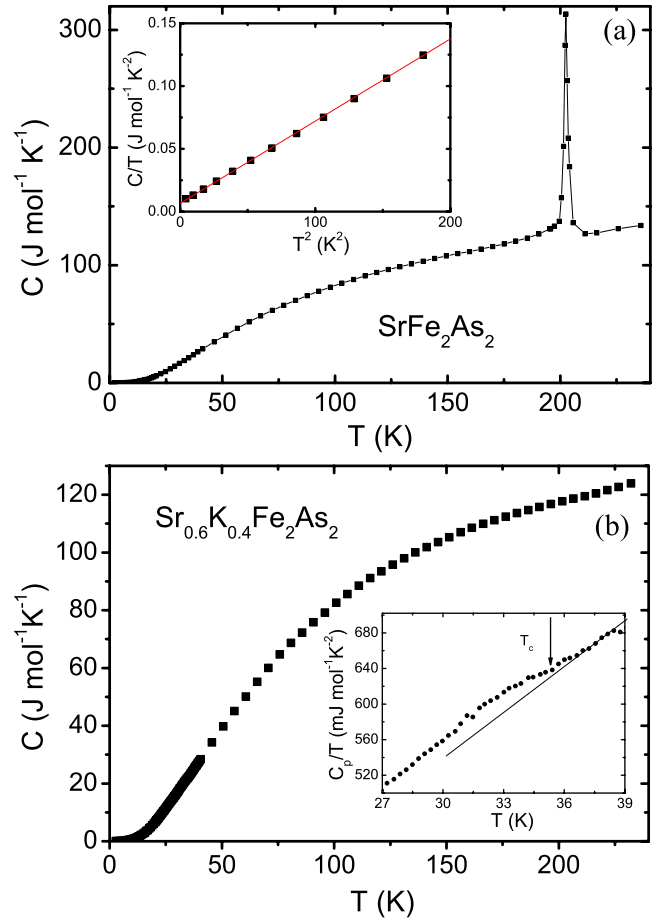


FIG. 4. (Color online) (a) Temperature dependence of specific heat C for SrFe_2As_2 . Inset: T^2 dependence of C/T in low temperatures. (b) Temperature dependence of specific heat C for $\text{Sr}_{0.6}\text{K}_{0.4}\text{Fe}_2\text{As}_2$. Inset: C/T around superconducting transition.

data, corresponding to structural and SDW transitions, respectively.³⁰ This suggests the structural transition and SDW transition occur at the same temperature in SrFe_2As_2 , similar to that observed in BaFe_2As_2 .^{18,19} At low temperatures, a good linear T^2 dependence of C/T is observed which indicates that the specific heat C is mainly contributed by electrons and phonons [see inset of Fig. 4(a)]. The fit yields the electronic coefficient $\gamma = 6.5$ mJ/mol K² and the Debye temperature $\theta_D = 245$ K. Note that the electronic coefficient is significantly smaller than the values obtained from the band-structure calculations for nonmagnetic state.³¹ This can be explained that a partial energy gap is opened below SDW transition; the smaller experimental value here could be naturally accounted for by the gap formation which removes parts of the density of states below the phase transition. Compared with band calculation, similar smaller electronic specific-heat coefficient was also observed in LaOFeAs due to gap opening originated from SDW instability.¹¹ In comparison, we also measured specific heat of superconducting crystal $\text{Sr}_{0.6}\text{K}_{0.4}\text{Fe}_2\text{As}_2$ prepared using FeAs as flux. It is found that no structural and SDW transitions can be observed in specific-heat data. Instead, a specific-heat anomaly at a superconducting transition temperature with $T_c \sim 35.6$ K is observed. The specific-heat jump $\Delta C/T_c$ is found to be ~ 48 mJ/mol K².

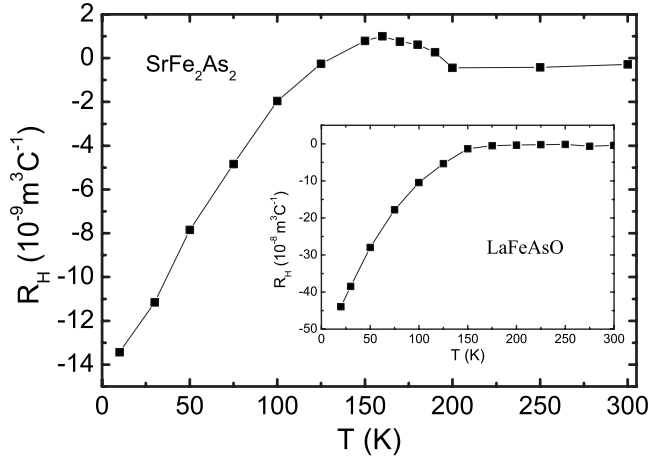


FIG. 5. Temperature dependence of Hall coefficient for SrFe_2As_2 . For comparison, the temperature dependence of Hall coefficient of LaFeAsO is shown in the inset.

Hall coefficient R_H as a function of temperature between 20 and 300 K for SrFe_2As_2 is shown in Fig. 5. For comparison, $R_H(T)$ for LaFeAsO is also shown in inset of Fig. 5. Above 200 K, the Hall coefficient is negative and nearly temperature independent for SrFe_2As_2 , indicating that conduction carriers are dominated by electrons. The carrier density is estimated as being $n=1.5 \times 10^{22} \text{ cm}^{-3}$ at 300 K if one-band model is simply adopted. It is nearly an order higher than that of LaFeAsO with $n \sim 1.8 \times 10^{21} \text{ cm}^{-3}$ at 300 K obtained by same method. Optical measurement also indi-

cates a quite large plasma frequency, $\omega_p \sim 1.5 \text{ eV}$.³² The large carrier number for SrFe_2As_2 indicates that it is a good metal. Below 200 K, the Hall coefficient increases slightly to a positive value, and then drops dramatically to a very large negative value. The absolute value of R_H at 2 K is about 35 times larger than that at 300 K. The dramatic change reflects the reconstruction of Fermi surface after SDW transition. The band calculations show that there are three hole pockets around Γ point and two electron pockets around M point.¹¹ The experiments seem to indicate that upon cooling below the SDW transition temperature, hole pockets are almost fully gapped while the electron pockets are partially gapped. Therefore, at low temperatures, the R_H reflect mainly the ungapped electron density around point M , which is significantly small in comparison with its initial value above 200 K.

In addition to parent SrFe_2As_2 , the anisotropy of resistivity and upper critical field for single crystals of $\text{A}_{0.6}\text{K}_{0.4}\text{Fe}_2\text{As}_2$ ($A=\text{Sr}, \text{Ba}$) is also investigated. Figure 6(a) shows the temperature dependence of the in-plane resistivity in zero field for $\text{Sr}_{0.6}\text{K}_{0.4}\text{Fe}_2\text{As}_2$ and $\text{Ba}_{0.6}\text{K}_{0.4}\text{Fe}_2\text{As}_2$ crystals. ρ_{ab} decreases with decreasing temperature and shows a downward curvature for $\text{Sr}_{0.6}\text{K}_{0.4}\text{Fe}_2\text{As}_2$, consistent with the polycrystal sample. With further decreasing temperature, an extremely sharp superconducting transition at 35.5 K with transition width of about 0.3 K is observed, indicating high homogeneity of the sample. A sharp superconducting transition for $\text{Ba}_{0.6}\text{K}_{0.4}\text{Fe}_2\text{As}_2$ is also observed with $T_c=38 \text{ K}$, slightly higher than that of $\text{Sr}_{0.6}\text{K}_{0.4}\text{Fe}_2\text{As}_2$. The anisotropic resistivity ρ_c/ρ_{ab} in normal state for $\text{Sr}_{0.6}\text{K}_{0.4}\text{Fe}_2\text{As}_2$ is found

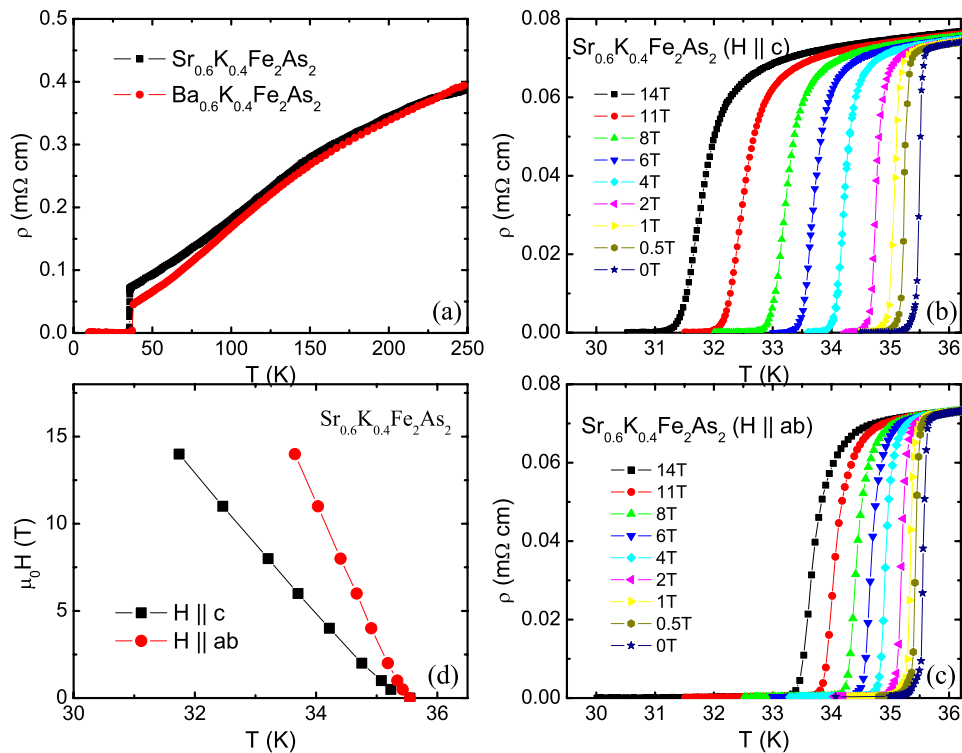


FIG. 6. (Color online) (a) Temperature dependence of the in-plane electrical resistivity for $\text{Sr}_{0.6}\text{K}_{0.4}\text{Fe}_2\text{As}_2$ and $\text{Ba}_{0.6}\text{K}_{0.4}\text{Fe}_2\text{As}_2$ in zero field. [(b) and (c)] Temperature dependence of the in-plane electrical resistivity for $\text{Sr}_{0.6}\text{K}_{0.4}\text{Fe}_2\text{As}_2$ at fixed fields of up to 14 T for $H \parallel c$ and $H \parallel ab$. (d) $H_{c2}(T)$ plot for $H \parallel c$ (closed square) and $H \parallel ab$ (open circle).

to be 21, much lower than that of parent SrFe_2As_2 .

Figures 6(b) and 6(c) show $\rho_{ab}(T)$ for $\text{Sr}_{0.6}\text{K}_{0.4}\text{Fe}_2\text{As}_2$ in external magnetic fields of up to 14 T along c axis and within ab plane, respectively. We can see that the superconducting transition is broadened slightly in magnetic fields of up to 14 T. The behavior is different from polycrystalline LaFeAsO where the superconducting transition is broadened strongly in magnetic fields.³³ Figure 6(d) shows H_{c2} - T_c curves for both $H\parallel ab$ and $H\parallel c$, respectively, where T_c is adopted by a criterion of 90% of normal-state resistivity. The curves $H_{c2}(T)$ are very steep with slopes $-dH_{c2}^{ab}/dT|_{T_c}=7.57$ T/K for $H\parallel ab$ and $-dH_{c2}^{ab}/dT|_{T_c}=3.80$ T/K for $H\parallel c$. This indicates that the upper critical fields are extremely high for $\text{Sr}_{0.6}\text{K}_{0.4}\text{Fe}_2\text{As}_2$. Using the Werthamer-Helfand-Hohenberg formula³⁴ $H_{c2}(0)=-0.69(dH_{c2}/dT)|_{T_c}$ and taking $T_c=35.5$ K, the upper critical fields are $H_{c2}^{ab}=185.4$ T and $H_{c2}^c=93.1$ T. The anisotropy ratio $\gamma=H_{c2}^{ab}/H_{c2}^c\approx 2.0$.²⁰ The value of γ is close to that of $\text{Ba}_{0.55}\text{K}_{0.45}\text{Fe}_2\text{As}_2$ with γ between 2.5 and 3.5. It is lower than that of F-doped NdFeAsO (Ref. 35) with $\gamma\approx 4.3-4.9$, and much lower than high- T_c cuprates; for example, $\gamma\approx 7-10$ for YBCO.³⁶ The lower values of ρ_c/ρ_{ab}

and γ indicate that the interplane coupling in $\text{Sr}_{0.6}\text{K}_{0.4}\text{Fe}_2\text{As}_2$ is relatively strong.

To summarize, SrFe_2As_2 and $\text{A}_{0.6}\text{K}_{0.4}\text{Fe}_2\text{As}_2$ ($A=\text{Sr}, \text{Ba}$) single crystals were prepared by flux method. The angular dependence of in-plane resistivity was measured for SrFe_2As_2 . A twofold symmetry of oscillations in AMR is observed at low temperatures which possibly indicates a stripe-type spin structure below SDW temperature. In K-doped $\text{A}_{0.6}\text{K}_{0.4}\text{Fe}_2\text{As}_2$ ($A=\text{Sr}, \text{Ba}$), the SDW instability is suppressed and instead superconductivity appears with T_c above 35 K. The upper critical field is rather high with $H_{c2}^{ab}=185.4$ T, while its anisotropy is rather low. The interplane coupling may play an important role in this material.

We acknowledge Z. D. Wang, T. Xiang, and Z. Fang for helpful discussions, and Q. M. Meng for help in experiments. This work was supported by the NSF of China, the Knowledge Innovation Project of the Chinese Academy of Sciences, and the 973 project of the Ministry of Science and Technology of China.

- ¹Y. Kamihara, T. Watanabe, M. Hirano, and H. Hosono, *J. Am. Chem. Soc.* **130**, 3296 (2008).
- ²G. F. Chen, Z. Li, D. Wu, G. Li, W. Z. Hu, J. Dong, P. Zheng, J. L. Luo, and N. L. Wang, *Phys. Rev. Lett.* **100**, 247002 (2008).
- ³X. H. Chen, T. Wu, G. Wu, R. H. Liu, H. Chen, and D. F. Fang, *Nature (London)* **453**, 761 (2008).
- ⁴Z.-A. Ren, J. Yang, W. Lu, W. Yi, X.-L. Shen, Z.-C. Li, G.-C. Che, X.-L. Dong, L.-L. Sun, F. Zhou, and Z.-X. Zhao, *Europhys. Lett.* **82**, 57002 (2008).
- ⁵C. Wang, L. Li, S. Chi, Z. Zhu, Z. Ren, Y. Li, Y. Wang, X. Lin, Y. Luo, X. Xu, G. Cao, and Z. Xu, *Europhys. Lett.* **83**, 67006 (2008).
- ⁶M. Rotter, M. Tegel, and D. Johrendt, *Phys. Rev. Lett.* **101**, 107006 (2008).
- ⁷G. F. Chen, Z. Li, G. Li, W. Z. Hu, J. Dong, X. D. Zhang, P. Zheng, N. L. Wang, and J. L. Luo, *Chin. Phys. Lett.* **25**, 3403 (2008).
- ⁸G. Wu, R. H. Liu, H. Chen, Y. J. Yan, T. Wu, Y. L. Xie, J. J. Ying, X. F. Wang, D. F. Fang, and X. H. Chen, *Europhys. Lett.* **84**, 27010 (2008).
- ⁹K. Sasmal, B. Lv, B. Lorenz, A. M. Guloy, F. Chen, Y. Y. Xue, and C. W. Chu, *Phys. Rev. Lett.* **101**, 107007 (2008).
- ¹⁰G. Wu, H. Chen, T. Wu, Y. L. Xie, Y. J. Yan, R. H. Liu, X. F. Wang, J. J. Ying, and X. H. Chen, *J. Phys.: Condens. Matter* **20**, 422201 (2008).
- ¹¹J. Dong, H. J. Zhang, G. Xu, Z. Li, G. Li, W. Z. Hu, D. Wu, G. F. Chen, X. Dai, J. L. Luo, Z. Fang, and N. L. Wang, *Europhys. Lett.* **83**, 27006 (2008).
- ¹²C. de la Cruz, Q. Huang, J. W. Lynn, J. Li, W. Ratcliff II, J. L. Zarestky, H. A. Mook, G. F. Chen, J. L. Luo, N. L. Wang, and Pengcheng Dai, *Nature (London)* **453**, 899 (2008).
- ¹³Y. Nakai, K. Ishida, Y. Kamihara, M. Hirano, and Hideo Hosono, *J. Phys. Soc. Jpn.* **77**, 073701 (2008).
- ¹⁴H.-H. Klauss, H. Luetkens, R. Klingeler, C. Hess, F. J. Litterst, M. Kraken, M. M. Korshunov, I. Eremin, S.-L. Drechsler, R. Khasanov, A. Amato, J. Hamann-Borrero, N. Leps, A. Kondrat, G. Behr, J. Werner, and B. Buchner, *Phys. Rev. Lett.* **101**, 077005 (2008).
- ¹⁵S. Kitao, Y. Kobayashi, S. Higashitaniguchi, M. Saito, Y. Kamihara, M. Hirano, T. Mitsui, H. Hosono, and M. Seto, *J. Phys. Soc. Jpn.* **77**, 103706 (2008).
- ¹⁶G. F. Chen, Z. Li, D. Wu, J. Dong, G. Li, W. Z. Hu, P. Zheng, J. L. Luo, and N. L. Wang, *Chin. Phys. Lett.* **25**, 2235 (2008).
- ¹⁷L. Ding, C. He, J. K. Dong, T. Wu, R. H. Liu, X. H. Chen, and S. Y. Li, *Phys. Rev. B* **77**, 180510(R) (2008).
- ¹⁸Q. Huang, Y. Qiu, Wei Bao, J. W. Lynn, M. A. Green, Y. Chen, T. Wu, G. Wu, and X. H. Chen, arXiv:0806.2776 (unpublished).
- ¹⁹M. Rotter, M. Tegel, D. Johrendt, I. Schellenberg, W. Hermes, and R. Pottgen, *Phys. Rev. B* **78**, 020503(R) (2008).
- ²⁰N. Ni, S. L. Bud'ko, A. Kreyssig, S. Nandi, G. E. Rustan, A. I. Goldman, S. Gupta, J. D. Corbett, A. Kracher, and P. C. Canfield, *Phys. Rev. B* **78**, 014507 (2008).
- ²¹J. Q. Yan, A. Kreyssig, S. Nandi, N. Ni, S. L. Bud'ko, A. Kracher, R. J. McQueeney, R. W. McCallum, T. A. Lograsso, A. I. Goldman, and P. C. Canfield, *Phys. Rev. B* **78**, 024516 (2008).
- ²²N. Ni, S. Nandi, A. Kreyssig, A. I. Goldman, E. D. Mun, S. L. Bud'ko, and P. C. Canfield, *Phys. Rev. B* **78**, 014523 (2008).
- ²³M. Tegel, M. Rotter, V. Weiss, F. M. Schappacher, R. Poettgen, and D. Johrendt, *J. Phys.: Condens. Matter* **20**, 452201 (2008).
- ²⁴J. Zhao, W. Ratcliff, J. W. Lynn, G. F. Chen, J. L. Luo, N. L. Wang, J. Hu, and P. Dai, *Phys. Rev. B* **78**, 140504(R) (2008).
- ²⁵T. A. Friedmann, M. W. Rabin, J. Giapintzakis, J. P. Rice, and D. M. Ginsberg, *Phys. Rev. B* **42**, 6217 (1990).
- ²⁶X. H. Chen, C. H. Wang, G. Y. Wang, X. G. Luo, J. L. Luo, G. T. Liu, and N. L. Wang, *Phys. Rev. B* **72**, 064517 (2005).
- ²⁷F. Hu, G. T. Liu, J. L. Luo, D. Wu, N. L. Wang, and T. Xiang, *Phys. Rev. B* **73**, 212414 (2006).
- ²⁸K. Kaneko, A. Hoser, N. Caroca-Canales, A. Jesche, C. Krellner,

- O. Stockert, and C. Geibel, arXiv:0807.2608 (unpublished).
- ²⁹X. F. Wang, T. Wu, G. Wu, H. Chen, Y. L. Xie, J. J. Ying, Y. J. Yan, R. H. Liu, and X. H. Chen, arXiv:0806.2452 (unpublished).
- ³⁰Michael A. McGuire, Andrew D. Christianson, Athena S. Sefat, Brian C. Sales, Mark D. Lumsden, Rongying Jin, E. A. Payzant, David Mandrus, Yanbing Luan, Veerle Keppens, Vijayalaksmi Varadarajan, Joseph W. Brill, Raphael P. Hermann, Moulay T. Sougrati, Fernande Grandjean, and Gary J. Long, *Phys. Rev. B* **78**, 094517 (2008).
- ³¹F. Ma, Z.-Y. Lu, and T. Xiang, arXiv:0806.3526 (unpublished).
- ³²W. Z. Hu, J. Dong, G. Li, Z. Li, P. Zheng, G. F. Chen, J. L. Luo, and N. L. Wang, arXiv:0806.2652 (unpublished).
- ³³G. F. Chen, Z. Li, G. Li, J. Zhou, D. Wu, J. Dong, W. Z. Hu, P. Zheng, Z. J. Chen, H. Q. Yuan, J. Singleton, J. L. Luo, and N. L. Wang, *Phys. Rev. Lett.* **101**, 057007 (2008).
- ³⁴N. R. Werthamer, E. Helfand, and P. C. Hohenberg, *Phys. Rev.* **147**, 295 (1966).
- ³⁵Y. Jia, P. Cheng, L. Fang, H. Q. Luo, H. Yang, C. Ren, L. Shan, C. Z. Gu, and H. H. Wen, *Appl. Phys. Lett.* **93**, 032503 (2008).
- ³⁶K. K. Nanda, *Physica C* **265**, 26 (1996).